Organic LETTERS

Letter

pubs.acs.org/OrgLett

Structural Characterization and Antioxidative Activity of Lancifonins: Unique Nortriterpenoids from *Schisandra lancifolia*

Yi-Ming Shi,[†,§,⊥] Jie Yang,[‡,⊥] Li Xu,[†,§] Xiao-Nian Li,[†] Shan-Zhai Shang,[†] Peng Cao,*[,‡] Wei-Lie Xiao,*[,†] and Han-Dong Sun*[,†]

[†]State Key Laboratory of Phytochemistry and Plant Resources in West China, Kunming Institute of Botany, Chinese Academy of Sciences, Kunming 650201, Yunnan, P. R. China

[‡]Laboratory of Cellular and Molecular Biology, Jiangsu Branch of China Academy of Traditional Chinese Medicine, Nanjing 210028, Jiangsu, P. R. China

[§]University of Chinese Academy of Sciences, Beijing 100049, P. R. China

Supporting Information

ABSTRACT: Six unique nortriterpenoids, lancifonins A−F (**1**−**6**), were isolated from *Schisandra lancifolia*. Their absolute configurations were determined by X-ray diffraction and ECD calculation. The conformational analysis of **1** was performed due to the unanticipated changes of Cotton effects in its ECD spectrum. Compounds **5** and **6** possess a unique 7/7 fused carbocyclic core with an internal ester bridge between C-9 and C-14, and **5** exhibited protective activity against H_2O_2-induced oxidative damage on Caco-2 cells.

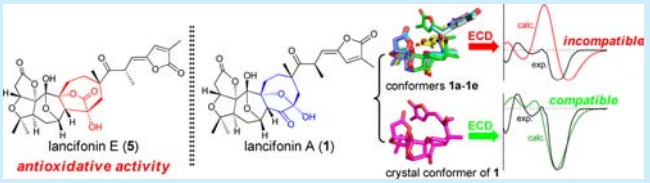

Plants of the *Schisandra* genus are rich sources of highly oxygenated and rearranged norcycloartane-type triterpenoids named schinortriterpenoids (SNTs).[1] The discovery of the first member of SNT micrandilactone A[2] in 2003 is a prelude to numerous research on this class of molecules in the fields of phytochemistry[1] and organic synthesis.[1,3] *Schisandra lancifolia* (Rehd. et Wils.) A. C. Smith, especially distributed in the Nujiang prefecture of Yunnan province in China, could be considered to be a prominent producer of novel SNTs,[4] which make this species eminently rewarding to systematic research. As a result of continuing investigation on architecturally interesting SNTs with bioactivities from this species, six unique and biogenetically related SNTs, lancifonins A−F (**1**−**6**), were discovered. Their absolute configurations were established by X-ray diffraction and ECD calculation. The ECD spectrum of **1** was serendipitously found to be a special case in SNTs, when compared to those of other (20*R*)-16,17-*seco*-preschisanartane-type SNTs. Therefore, its conformational analysis was performed. Most notably, **5** and **6** possess an unprecedented rearranged carbocyclic core with an internal ester bridge between C-9 and C-14. In addition, compound **5** exhibited protective activity against H_2O_2-induced oxidative damage on Caco-2 cells with an EC_{50} value of 0.26 mM. Herein, we report the structural elucidation, including absolute configurational and conformational analysis, and the antioxidative activities of **1**−**6**.

Compound **1** had a molecular formula of $C_{29}H_{34}O_{11}$, as determined by ESIMS and HREIMS (*m*/*z* 558.2110, calcd 558.2101). The NMR spectra of **1** (Tables S1 and S2, Supporting Information) closely resembled schisdilactone E,[5] except for C-7, C-19, and C-29. The presence of an oxa-bridged hemiketal in the seven-membered carbon ring of **1** was

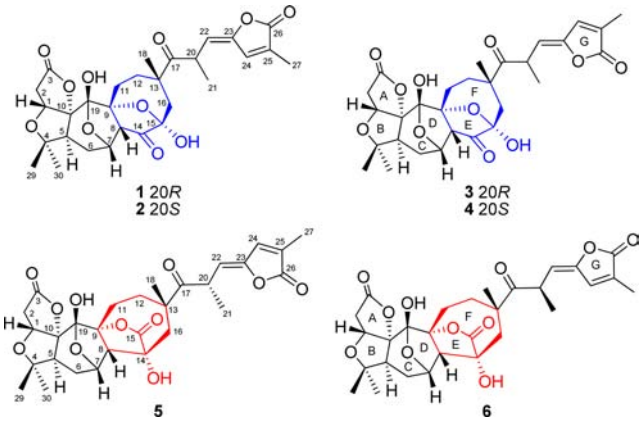

supported by the HMBC correlation from an oxymethine (H-7, δ_H 4.50) to a hemiketal group (C-19, δ_C 104.8). An oxymethylene attached at C-4 in schisdilactone E was replaced by a methyl (C-29, δ_C 25.3) in **1**, which was judged by the HMBC correlations from Me-29 (δ_H 1.14) to C-4 (δ_C 85.7) and C-30 (δ_C 30.3). Finally, the absolute configuration of **1** was determined to be 1*R*, 5*S*, 7*S*, 8*R*, 9*R*, 10*R*, 13*S*, 15*S*, 19*S*, and 20*R* by X-ray diffraction using Cu Kα radiation [Flack parameter = 0.11(11)][6] (Figure 1). Full structural elucidation of **2**−**4** by NMR, MS, and ECD could be readily performed.[7]

It has previously been reported that the absolute configurational assignment for C-20 of 16,17-*seco*-preschisanartane-type SNTs featuring an $\alpha,\beta,\gamma,\delta$-unsaturated-$\gamma$-lactone moiety and a carbonyl group in the side chain could be provided by the

Received: January 15, 2014
Published: February 19, 2014

   dx.doi.org/10.1021/ol5001186 | *Org. Lett.* 2014, 16, 1370−1373

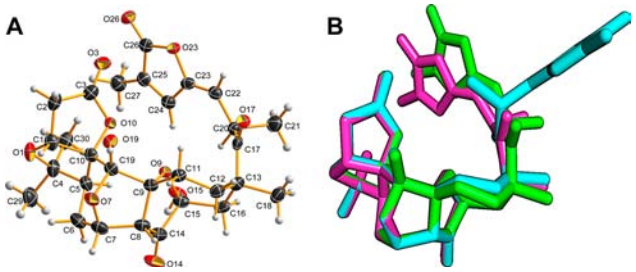

Figure 1. (A) X-ray crystallographic structure of compound **1**. (B) Overlay of higher-energy conformer (**1a**, green), lowest-energy conformer (**1c**, blue), and the crystal conformer (**1**, pink).

diagnostic positive Cotton effect (CE) around 310 nm and negative CE around 275 nm for 20*S* as well as the diagnostic negative CE around 310 nm and positive CE around 275 nm for 20*R* in ECD spectrum.[5,8] Although the absolute configuration for C-20 of **1** was assigned to be *R* by X-ray diffraction, the experimental ECD spectrum of **1**, which was characterized by only one intense negative CE at 301 nm, was significantly distinct from those of other (20*R*)-16,17-*seco*-preschisanartane-type SNTs.[5,8] It could be therefore postulated that the solution conformational characteristics of **1** were responsible for its abnormal variations of CEs in its ECD spectrum.[9] Subsequently, conformational analysis and theoretical ECD calculation were performed, in order to evaluate the solution conformers of **1**. Unfortunately, the Boltzmann-weighted ECD spectrum of **1** calculated by the TDDFT method at the B3LYP-SCRF/6-31+G(d,p)//B3LYP/6-31G(d) level with PCM in methanol was also incompatible with the experimental one (Figure 2), which might result from the

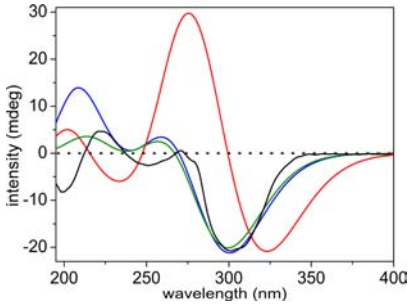

Figure 2. Experimental ECD of **1** (black), Boltzmann-weighted ECD of **1** (red), calculated ECD of conformer **1a** (blue), and calculated ECD of the crystal conformer of **1** (green).

failure to obtain the accurate evaluation of Bolzmann population and the lowest-energy conformer via B3LYP/6-31G(d). Although larger basis sets and different functionals, i.e., B3LYP/6-31+G(d,p), B3LYP/TZVP, and B97D/TZVP, were performed to reoptimize all the conformers in methanol solvent, their Boltzmann population and the lowest-energy conformer were almost the same as those obtained by B3LYP/6-31G(d) in the gas phase (Tables S4−S7). Under the circumstances, we analyzed the calculated ECD spectrum of each conformer (**1a**−**1e**) and found that only the minor conformer **1a** (0.8, 0.4, 0.6, 6.0, and 12.9% obtained at different levels, Tables S4−S7) generated an ECD curve similar to the experimental one (Figures 2 and S1). In addition, **1a** conformationally resembled the crystal conformer of **1** while the predominant conformer **1c** (78.7, 94.6, 86.4,85.2, and 81.5% obtained at different levels, Tables S4−S7) showed significant differences from **1a** and the crystal conformer of **1**, pertaining to the C_9 side chains (Figure 1B). Finally, the ECD spectrum of the crystal conformer of **1** was calculated at the B3LYP-SCRF/6-31+G(d,p)//B3LYP/6-31G(d) level with PCM in methanol, which afforded extremely good agreement with the experimental one (Figure 2). Thus, this evidence suggested that the steric structure of **1** in crystal was also predominantly preserved in methanol.

Inspection of conformer **1a**, the crystal conformer of **1**, and conformer **1c** had showed that an intramolecular hydrogen bond, 15O−H···O═C14, was present in the former two conformers, while 15O−H···O═C17 existed in conformer **1c** instead (Figure S2). Furthermore, the hydrogen bond length and bond angles of conformer **1a** were close to those of the crystal conformer of **1** (Figure 3). As a result, the intra-

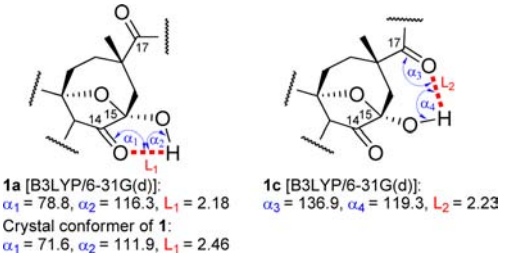

Figure 3. Intramolecular hydrogen bonds (red dash) of conformer **1a**, the crystal conformer of **1**, and conformer **1c** and corresponding bond angles (deg) and bond lengths (Å) obtained by calculation and X-ray diffraction.

molecular hydrogen bonding of OH-15 with the carbonyl group at C-14 or C-17 could be one of the main reasons for conformational alterations of the flexible side chain, which led to the unanticipated but remarkable variations of CEs.

Lancifonin E (**5**) had a molecular formula of $C_{29}H_{34}O_{11}$, as determined by positive ESIMS and HREIMS (*m*/*z* 558.2101, calcd 558.2101), requiring 13 degrees of unsaturation. By analysis of the HSQC spectrum, all protons signals were assigned to their respective carbons unambiguously except for two signals at δ_H 5.22 and 6.08, which suggested that these two protons were from two hydroxy groups. Detailed comparison of the 1D NMR spectra of **5** with those of **1** (Tables S1 and S2) suggested that the substructures of rings A−D and C_9 side chain remained intact in **5**. However, it was obvious that the characteristic signals for **1** at C-9 (δ_C 89.8), C-14 (δ_C 211.7), and C-15 (δ_C 105.8) were absent in **5**. Instead, the existence of three anomalous quaternary carbons at δ_C 75.2, 91.9, and 177.8 were observed. Therefore, the observed differences could be rationalized by the rearrangement of the eight-membered carbon ring in **5**. The hydroxy group at δ_H 5.22 was located at C-14 (δ_C 75.2) on the basis of the HMBC correlations (Figure 4) from OH-14 to C-8 (δ_C 53.4), C-14, and C-16 (δ_C 48.4). C-8 attached to C-16 through an oxygenated quaternary carbon at δ_C 75.2 was judged from the HMBC correlations from H-8 (δ_H 3.13) to C-14 and C-16 and the aforementioned HMBC correlations of OH-14. Meanwhile, the HMBC correlations from H-11β (δ_H 2.07) and H-12α (δ_H 2.18) to C-9 and from Me-18 to C-12, C-13, and C-16, together with the $^1H-^1H$ COSY and HSQC-TOCSY correlations of H_2-11/H_2-12, established the unique seven-membered carbon ring that consisted of C-8, C-9, C-11, C-12, C-13, C-14, and C-16. An ester group (δ_C 177.8), namely C-15, was attached to C-14,

dx.doi.org/10.1021/ol5001186 | *Org. Lett.* 2014, 16, 1370−1373

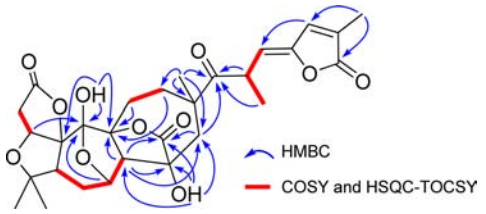

Figure 4. Key HMBC, ^{1}H−^{1}H COSY, and HSQC-TOCSY correlations of **5**.

which was supported by the HMBC correlations from H-8, OH-14, and H_2-16 to C-15. Finally, there was still 1 degree of unsaturation unaccounted for, requiring another ring in the final structure. When the chemical shift of C-9 in **5** was compared with that of **1**, the downfield chemical shift of C-9 in **5** indicated it to be esterified and therefore C-15 had to be connected to the oxygen left (O-9) through an ester bond. Thus, the planar structure of **5** was established.

The relative configuration of the stereogenic centers in rings A−D of **5** was determined to be the same as those in **1** by the similar ROESY correlations (Figure 5) and carbon and proton

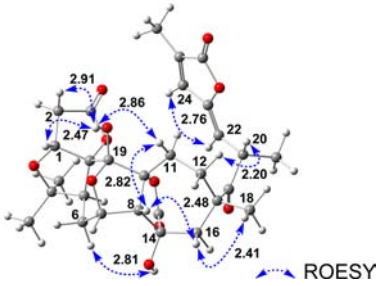

Figure 5. Key ROESY correlations of **5** and corresponding interatomic distance (Å).

chemical shifts of both compounds (Tables S1 and S2). In addition, the ester bridge between C-9 and C-14 in **5** was *α*-oriented, judging from the ROESY correlations of H-8 with H-11*β* (δ_H 2.07) and H-16*β* (δ_H 1.87), of OH-14 with H-6*α* (δ_H 2.09), and of H-16*β* with Me-18 (δ_H 1.18). In addition, the double bond between C-22 and C-23 was in a *Z* geometry, which was supported by the ROESY correlation from H-22 (δ_H 4.89) to H-24 (δ_H 7.33). These observations were all supported by DFT calculation of the predominant conformer **5e** (85.8%) that was optimized at the B3LYP/6-31G(d) level (Figure 5).

The absolute configuration of C-20 was established by calculated ECD spectra of C-20 epimers for **5**. The comparison of the experimental ECD spectrum with the calculated ECD spectra for (20*S*)-**5** and (20*R*)-**5** was shown (Figure 6). Overall, the calculated ECD spectra for (20*S*)-**5** showed diagnostic positive and negative CEs at 316 and 280 nm, respectively, consistent with the experimental one. Thus, the absolute configuration of C-20 in **5** was assigned as *S*. Molecular orbital (MO) analysis used the predominant conformer **5e** as an example to afford a thorough understanding of the experimental ECD curve of **5** (Figure S3).

Careful comparison of the NMR data of **6** with those of **5** (Tables S1 and S2) obviously suggested that **6** was another SNT structurally similar to **5**. The double bond between C-22 and C-23 of **6** was determined to be in an *E* geometry, which was supported by the ROESY correlation of H-20 (δ_H 4.23) with H-24 (δ_H 7.96) and the disappearance of the correlation of

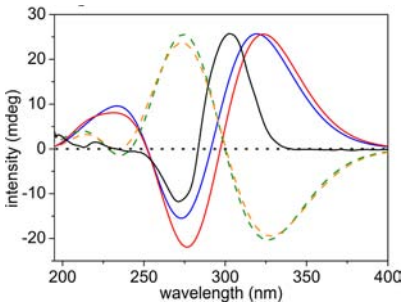

Figure 6. Experimental ECD spectrum of **5** (black), calculated ECD spectra of (20*S*)-**5** in the gas phase (blue) and in methanol (red), and calculated ECD spectra of (20*R*)-**5** in the gas phase (orange) and in methanol (green).

H-22 (δ_H 5.49) with H-24.[10] In addition, the absolute configuration of C-20 in **6** was demonstrated to be *R* by an empirical comparison of its experimental ECD spectrum to that of **5**.

The 7/8 fused carbocyclic core with an oxa-bridged ketal/hemiketal in the eight-membered carbon ring is an intact substructure (Scheme 1 in blue), especially preserved in

Scheme 1. Hypothetical Biogenetic Pathway of 5

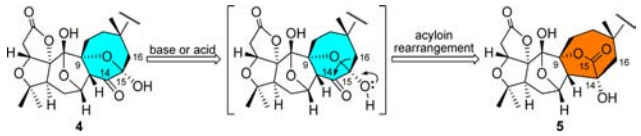

schisanartane, preschisanartane, and 16,17-*seco*-preschisanartane-type SNTs.[1,5,8] From a literature research, only arisandilactone A has hitherto been reported to possess a 7/9 fused carbocyclic core that expanded from a 7/8 fused ring system.[11] In contrast to arisandilactone A, the unique 7/7 core skeleton of **5** and **6** presumably arises from the 7/8 backbone via a ring-contraction process, namely acyloin rearrangement (Scheme 1).[12] On the basis of biogenetic considerations and the X-ray crystallographic structure of **1**, the same absolute configuration of the western hemisphere is suggested for compounds **1**−**6**.

Oxidative damage at the cellular level is closely related to multiple human diseases, such as cancer and neurodegeneration.[13] Dibenzocyclooctene lignans, the major component in plants of Schisandraceae family, are known to have a potent antioxidative effect,[14] but such pharmacological knowledge of the minor constituents, SNTs, is still unknown. It is interesting to explore whether such highly oxygenated molecules possess an antioxidative property. Thus compounds **1**−**5**, except **6** due to sample quantity limitation, were evaluated for their protective activities against H_2O_2-induced oxidative damage on Caco-2 cells. Compounds **1**−**4** showed weak activity while **5** exhibited protective efficacy with an EC_{50} value of 0.26 mM, which was better than those of the positive controls *N*-acetyl-L-cysteine (EC_{50} = 4.2 mM) and *γ*-Glu-Cys-Gly (EC_{50} = 3.6 mM). It was observed that **5** promoted a significant increase in the number of survival Caco-2 cells (Figure 7). Furthermore, Hoechst 33258 staining was used to demonstrate that **5** could protect H_2O_2-induced Caco-2 cells against apoptosis (Figure 8). The apoptosis rate of H_2O_2-treated Caco-2 cells reduced from 50.4% in a negative control to 21.4% and 27.1% by pretreating the cells with **5** at 50 and 100 *μ*M, respectively

dx.doi.org/10.1021/ol5001186 | *Org. Lett.* 2014, 16, 1370−1373

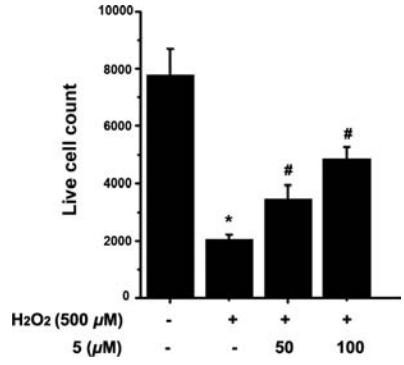

Figure 7. Live cell count per 96 well were determined after Caco-2 cells were stimulated by H_2O_2 with or without pretreatment of different concentrations of **5** (*p < 0.05 vs control, #p < 0.05 vs H_2O_2 treatment alone).

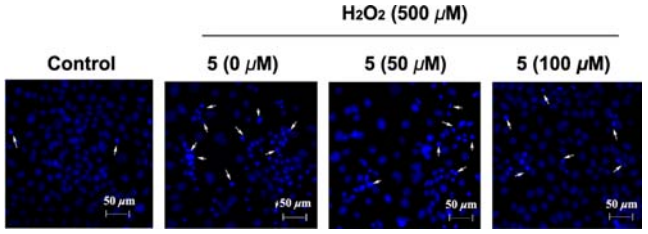

Figure 8. Protective activity of **5** against H_2O_2-induced Caco-2 cells apoptosis. Nuclear staining of Caco-2 cells with Hoechst 33258; apoptotic cells showed smaller nuclei with brilliant blue staining (white arrows).

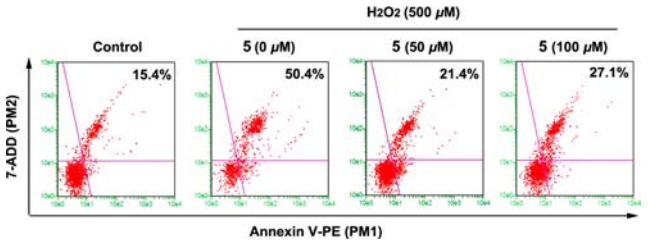

Figure 9. Apoptosis rate of H_2O_2-treated Caco-2 cells with or without pretreatment of different concentrations of **5**.

(Figure 9). It was found that phosphorylation of JNK1/2/3 MAPK in H_2O_2-treated Caco-2 cells was blocked by **5** (Figure S4), suggesting that this protective effect was correlated with a JNK pathway. The protective effect of **5**, when compared to those of **1**−**4**, indicated that the seven-membered carbon ring (rings E and F) with an internal ester bridge might be a structural requirement for activity. These results indicated that some modified SNTs may function as protective agents against oxidative damage, which shed new light onto the biological study of SNTs.

■ ASSOCIATED CONTENT

Supporting Information

Detailed experimental procedures, physical−chemical properties, 1D and 2D NMR, MS, IR, UV, and ECD spectra for compounds **1**−**6**, X-ray crystal structure (CIF) for compound **1**, and ECD calculation details for compounds **1** and **5**. This material is available free of charge via the Internet at http://pubs.acs.org.

■ AUTHOR INFORMATION

Corresponding Authors

*E-mail: pcao79@yahoo.com.
*E-mail: xwl@mail.kib.ac.cn.
*E-mail: hdsun@mail.kib.ac.cn.

Author Contributions

⊥These authors contributed equally.

Notes

The authors declare no competing financial interest.

■ ACKNOWLEDGMENTS

This project was supported financially by the NSFC (81373290 and 81274150), a CAS grant (KSCX2-EW-Q-10), and the NSFYP (2012FB178) and sponsored by SRF for ROCS, SEM to W.-L.X. The calculation sections were supported by HPC Center of Kunming Institute of Botany, CAS.

■ REFERENCES

(1) Xiao, W. L.; Li, R. T.; Huang, S. X.; Pu, J. X.; Sun, H. D. *Nat. Prod. Rep.* **2008**, *25*, 871−891.
(2) Li, R. T.; Zhao, Q. S.; Li, S. H.; Han, Q. B.; Sun, H. D.; Lu, Y.; Zhang, L. L.; Zheng, Q. T. *Org. Lett.* **2003**, *5*, 1023−1026.
(3) (a) Goh, S. S.; Baars, H.; Gockel, B.; Anderson, E. A. *Org. Lett.* **2012**, *14*, 6278−6281. (b) Bartoli, A.; Chouraqui, G.; Parrain, J. L. *Org. Lett.* **2012**, *14*, 122−125. (c) Xiao, Q.; Ren, W. W.; Chen, Z. X.; Sun, T. W.; Li, Y.; Ye, Q. D.; Gong, J. X.; Meng, F. K.; You, L.; Liu, Y. F.; Zhao, M. Z.; Xu, L. M.; Shan, Z. H.; Shi, Y.; Tang, Y. F.; Chen, J. H.; Yang, Z. *Angew. Chem., Int. Ed.* **2011**, *50*, 7373−7377. (d) Maity, S.; Matcha, K.; Ghosh, S. *J. Org. Chem.* **2010**, *75*, 4192−4200. (e) Cordonnier, M. C. A.; Kan, S. B. J.; Anderson, E. A. *Chem. Commun.* **2008**, 5818−5820.
(4) (a) Shi, Y. M.; Wang, X. B.; Li, X. N.; Luo, X.; Shen, Z. Y.; Wang, Y. P.; Xiao, W. L.; Sun, H. D. *Org. Lett.* **2013**, *15*, 5068−5071. (b) Luo, X.; Chang, Y.; Zhang, X. J.; Pu, J. X.; Gao, X. M.; Wu, Y. L.; Wang, R. R.; Xiao, W. L.; Zheng, Y. T.; Lu, Y.; Chen, G. Q.; Zheng, Q. T.; Sun, H. D. *Tetrahedron Lett.* **2009**, *50*, 5962−5964.
(5) Wang, J. R.; Kurtán, T.; Mándi, A.; Guo, Y. W. *Eur. J. Org. Chem.* **2012**, 5471−5482.
(6) Flack, H. D.; Bernardinelli, G. *Acta Crystallogr., Sect. A* **1999**, *55*, 908−915.
(7) For detailed structural elucidation of compounds **2**−**4**, see the Supporting Information.
(8) Shi, Y. M.; Li, X. Y.; Li, X. N.; Luo, X.; Xue, Y. B.; Liang, C. Q.; Zou, J.; Kong, L. M.; Li, Y.; Pu, J. X.; Xiao, W. L.; Sun, H. D. *Org. Lett.* **2011**, *13*, 3848−3851.
(9) Berova, N.; Di Bari, L.; Pescitelli, G. *Chem. Soc. Rev.* **2007**, *36*, 914−931.
(10) He, F.; Li, X. Y.; Yang, G. Y.; Li, X. N.; Luo, X.; Zou, J.; Li, Y.; Xiao, W. L.; Sun, H. D. *Tetrahedron* **2012**, *68*, 440−446.
(11) Cheng, Y. B.; Liao, T. C.; Lo, I. W.; Chen, Y. C.; Kuo, Y. C.; Chen, S. Y.; Chien, C. T.; Shen, Y. C. *Org. Lett.* **2010**, *12*, 1016−1019.
(12) (a) Song, Z. L.; Fan, C. A.; Tu, Y. Q. *Chem. Rev.* **2011**, *111*, 7523−7556. (b) Rosales, A.; Estevez, R. E.; Cuerva, J. M.; Oltra, J. E. *Angew. Chem., Int. Ed.* **2004**, *44*, 319−322.
(13) Halliwell, B. *Nutr. Rev.* **2012**, *70*, 257−265.
(14) (a) Chang, J. B.; Reiner, J.; Xie, J. X. *Chem. Rev.* **2005**, *105*, 4581−4609. (b) Hancke, J. L.; Burgos, R. A.; Ahumada, F. *Fitoterapia* **1999**, *70*, 451−471.